



HAL
open science

Development of a pre-chamber for ultra-lean operation of gasoline engines

Knut Habermann, Bastian Morcinkowski, Christoph Müller, Christof Schernus, Tolga Uhlmann

► **To cite this version:**

Knut Habermann, Bastian Morcinkowski, Christoph Müller, Christof Schernus, Tolga Uhlmann. Development of a pre-chamber for ultra-lean operation of gasoline engines. Proceedings of 8th Transport Research Arena TRA 2020, April 27-30, 2020, Helsinki, Finland, Apr 2020, Helsinki, Finland. hal-02504571

HAL Id: hal-02504571

<https://hal.science/hal-02504571>

Submitted on 10 Mar 2020

HAL is a multi-disciplinary open access archive for the deposit and dissemination of scientific research documents, whether they are published or not. The documents may come from teaching and research institutions in France or abroad, or from public or private research centers.

L'archive ouverte pluridisciplinaire **HAL**, est destinée au dépôt et à la diffusion de documents scientifiques de niveau recherche, publiés ou non, émanant des établissements d'enseignement et de recherche français ou étrangers, des laboratoires publics ou privés.



Proceedings of 8th Transport Research Arena TRA 2020, April 27-30, 2020, Helsinki, Finland

Development of a pre-chamber for ultra-lean operation of gasoline engines

Knut Habermann^{a*}, Bastian Morcinkowski^a, Christoph Müller^b, Christof Schernus^a,
Tolga Uhlmann^a

^aFEV Europe GmbH, Neuenhofstrasse 181, 52078 Aachen, Germany

^bVKA at Aachen University, Forckenbeckstraße 4, 52074 Aachen, Germany

Abstract

Combustion engines in hybridized powertrains continue to require further reductions in fuel consumption and emissions. Lean operation represents a major step towards increasing gasoline engine efficiency. Here, pre-chamber jet ignition offers the potential to assure a reliable ignition and combustion process. This paper describes the development of such a system. Numerical approaches allow for an efficient development process of the pre-chamber layout. Thus, the pre-chamber geometry is thoroughly optimized with respect to the combustion quality. Based thereupon, different pre-chamber layouts were experimentally evaluated. Optical investigations serve to conclude on burn rate and particulate emissions. Having found a specific layout to achieve stable combustion ($COV < 1.5\%$) for lean ($\lambda > 3$) operation and specific NO_x emissions below 0.1 g/kWh a synthesis of all findings serves to define the final concept. The resulting combustion system offers high efficiencies in the entire engine map and thus excellent conditions for further improving the fuel consumption.

Keywords: Gasoline engine; Pre-chamber ignition; Lean burn; Efficiency

* Corresponding author. Tel.: +49-241-5689-532;
E-mail address: habermann@fev.com

1. Introduction

Pre-chamber jet ignition represents an attractive approach for a lean burn engine concept in hybridized powertrains. Such system supplies a large quantity of turbulent hot gas to the main combustion chamber to ignite the highly diluted mixture. Hence, it is one of the space-igniting techniques [Böwing, Bunce, Sens]. It offers the potential to assure a reliable ignition and a stable combustion process. The development of such systems seeks intense frontloading by means of simulation and supportive optical investigations during thermodynamic experimental phase on a single cylinder engine.

The mixture in a pre-chamber can be realized either through scavenging mixture from the main chamber during the compression stroke (passive pre-chamber) or through additional external fuel feeding (active pre-chamber). The dosing can be done either by a check valve, commonly used in commercial gas engines, or by a separate injector. Active pre-chambers can be supplied with either liquid or gaseous fuels which have some advantages with regard to mixture formation. For the fuel supply to an active pre-chamber there are examples using fuel vapor [Schumacher], a pre-mixed fuel / air mixture [Böwing, Sens], methane [Böwing] or hydrogen [Lumsden].

2. Methodology

2.1. Charge Motion Development for Ultra Lean Combustion

An engine concept was developed to achieve high efficiencies for extremely lean mixtures. Usually, such concepts already make use of new approaches at the conventional ignition system. For example, by increasing the stroke-to-bore ratio, removing compression volume from the flame deck resulting in aerodynamically optimized high compression ration piston crowns, ports with maximum charge movement and modern DI injection systems.

For the development of such a layout, engineering processes are used which relate the thermodynamic state, the mixture formation and the flow characteristic from CFD simulations to combustion parameters. At least the combustion duration should be estimated; an additional prediction of the ignition or stability limits and the emissions is more accurate. These development tools are already state of the art for engines with conventional ignition systems like described by Wiese et al.

The main feature of the engine concept discussed in this paper is an active pre-chamber including a spark-plug and a fuel injector which enables an efficient combustion process in extreme diluted condition.

In the following a pragmatic approach - consisting of existing and newly developed methodologies - will be applied to support the development of such a combustion system.

2.2. Combustion modeling

A combination of numerical approaches with various levels of detail was used to layout the combustion system of the engine. 0D models based on multi-zone combustion were used to evaluate pre-chamber geometries with respect to the operating conditions, their volumes and hole configuration. This model is based on Auer et al. and describes both thermodynamic systems, the pre- and main combustion chamber, as well as the characteristics resulting from the turbulent hot ignition jets. The turbulence model of the main combustion chamber takes into account the mass entering from the pre-chamber, as well as the terms for turbulence by compression, squish effects and dissipation:

$$\frac{dk}{dt} = \frac{dk_{\text{compression}}}{dt} + \frac{dk_{\text{squish}}}{dt} + \frac{C_{\text{hole}} v_{\text{hole}}^2}{2 m_{\text{main}}} \frac{dm_{\text{hole}}}{dt} \quad (1)$$

The mass transfer is represented by empirical orifice models.

The calculation of the turbulent flame velocity for pre-chamber and main combustion chamber can be determined according to Peters and considers in addition to thermodynamic and mixture quantities also the turbulence:

$$\frac{s_T - s_L}{v'} = \frac{a_4 b_3^2}{2b_1} \text{Da} + \sqrt{\left(\frac{a_4 b_3^2}{2b_1} \text{Da}\right)^2 + a_4 b_3^2 \text{Da}} \quad (2)$$

For both combustion chambers, the flame front surface is stored map-based depending on the flame sphere diameter as proposed by Grill et al. Using reactive 3D computational fluid dynamics (CRFD), the spatially resolved mixture and turbulence distribution in the pre- and main combustion chamber are considered. In order to keep the computing effort reasonable, a multi-zone combustion model is used, which calculates the reaction kinetics in a representative phase space.

The concept of "zoning" and "mapping" according to Babajimopoulos et al., which is available in many commercial programs, is used for solving heat release and changes in the composition of chemical species: "Zoning" is used to classify individual cell values into different zones. This phase space is built up for each time step with the dimensions temperature and air-fuel ratio. The heat release and mixture composition calculated in each of these zones is again transferred to the CFD cells in the subsequent "mapping".

2.3. Coupled development process

In a first step, promising designs were derived from a wide range of possible chamber parameters using the presented 0D model. The design in 3D is then realized using the CRFD simulations.

The 3D simulations are based on thermodynamic boundary conditions from the 0D modelling. In turn, the empirical turbulence modeling in 0D is replaced by resolved turbulence data from CRFD. Usually one iteration is sufficient to achieve a convergent result.

3. Results

3.1. Simulation

The simulations have shown that the technical realizable design volumes between 1000 mm³ and 1600 mm³ in combination with 4 or 6 holes should lead to a stable ignition. Figure 1 shows for a small (1080 mm³) and a large (1611 mm³) chamber volume the initial pre-optimized CRFD designs.

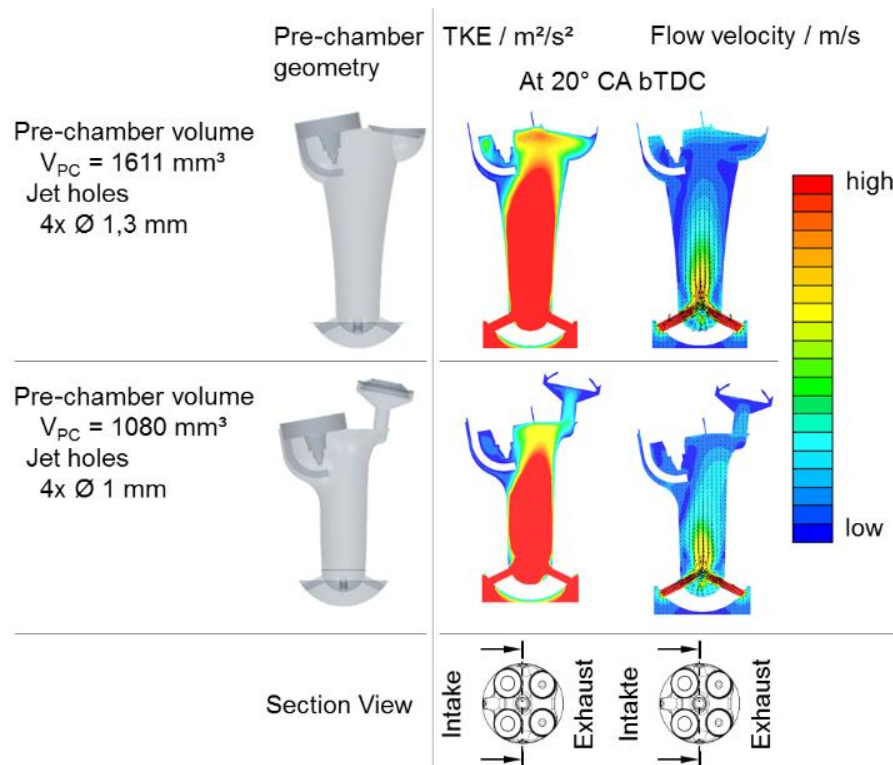


Figure 1 Pre-optimized 4-hole pre-chamber designs mainly based on initial 0D model layout and design boundaries

Considering the inflow, the central point where the flows meet leads to a strong dissipation resulting in high turbulence levels. The velocity in the upper part of the pre-chamber, where the spark plug is located, decreases strongly. However, at this point higher flow velocities and turbulence levels would be desirable to support ignition and early combustion.

Therefore, a detailed optimization was carried out with the following specifications

- A vertically offset swirl arrangement of the holes to generate a stable vortex in the chamber which dissipates mainly through geometric obstacles.
- A change in the shape that is more flow-favorable in the lower area and just dissipative in the upper area.

- A rearrangement of the spark plug to ensure a stable deflection of the ignition spark and a high turbulence level in the ignition gap.

Figure 2 shows the results of this optimized design. The advantages are clearly visible and independent from the pre-chamber volume. In addition, mixture formation analysis has been incorporated for the final verification of the pre-chamber. Results can be found in Serrano et al.

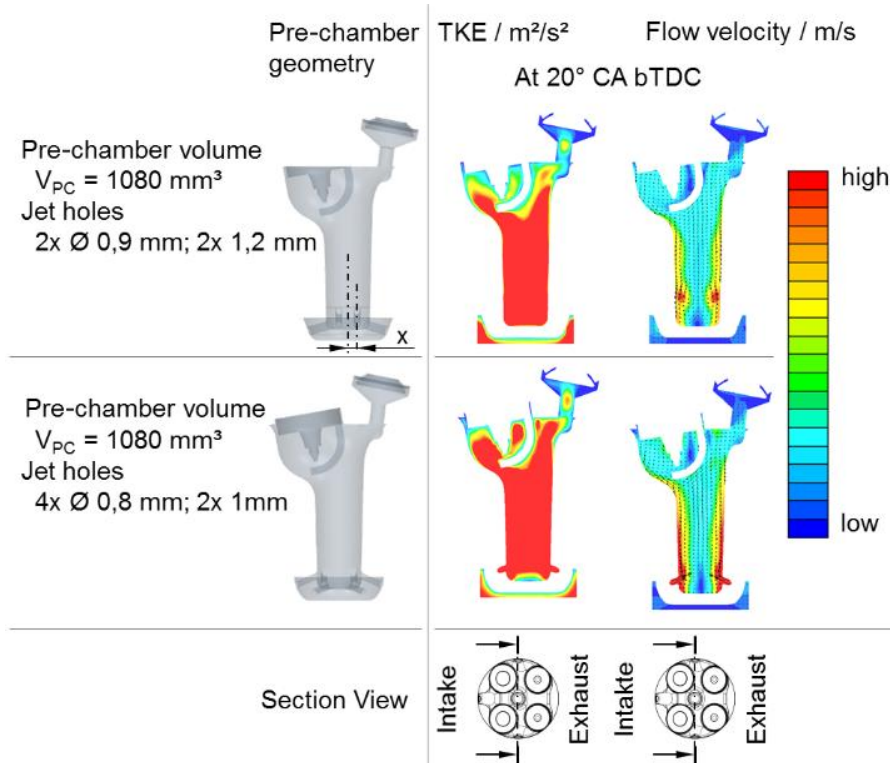


Figure 2 Optimized 4-hole pre-chamber designs resulting from 3D CRFD analysis

3.2. Single Cylinder Engine Testing

Based on the optimizations of the pre-chamber layout shown, tests were carried out on a single cylinder engine. A significant number of different air/fuel ratio sweeps have been performed to understand working principle better and to identify optimal operating strategy. Engine maps are created by selection the operation points from various lean-burn investigations for the best efficiency and lowest NO_x emissions.

The engine maps shown in Figure 3 and Figure 4 serve, on the one hand, to illustrate the results of an extreme lean-burn combustion process in terms of efficiency and emissions that can be achieved with the pre-chamber ignition system. In addition, the characteristic maps can be used to gain further insights into the function and boundary conditions for the design of an engine architecture.

In order to generate a fuel consumption-optimized characteristic map, the measuring points with the optimum efficiency for the respective operating point are selected from the lean-burn loops with different natural gas mass flows. The points selected on the basis of this criterion all show very good combustion stability with low cyclic fluctuations of the indicated mean pressure (COV_{imep} is for the most part below 1 %), Figure 3. Hence, all operating points show a clear distance to the lean-burn limit. The resulting efficiency map reaches the optimum of 43.9 % at $n = 2000 \text{ rpm}$ and $\text{imep} = 15 \text{ bar}$. The efficiency is lowered primarily with reduced load and to a minor extent also with increasing speed.

The selection of the operating points shows a pre-chamber fuel mass fraction decreasing with speed from more than 10 % at $n = 2000 \text{ rpm}$, $\text{imep} = 15 \text{ bar}$ down to 3.4 % at $n = 4000 \text{ rpm}$, $\text{imep} = 16 \text{ bar}$. As the load decreases, the pre-chamber fuel mass fraction decreases slightly and rises significantly again to very low loads due to a certain basic pre-chamber enrichment requirement.

The nitrogen oxide (NO) emissions for operating points of maximum efficiency are between 0.17 g/kWh and 0.51 g/kWh. These emissions, which also increase with engine speed, occasionally show islands of differing emission

formation. For the engine map with minimal NO emissions, the indicated specific NO emissions are, with one exception, between 0.14 g/kWh and 0.28 g/kWh, and are thus significantly lower than those of the engine map with maximum efficiency. Particularly with regard to the pre-chamber fuel mass fraction, the two engine maps differ clearly. The proportion of pre-chamber fuel lies between only 2 and 5 % in wide areas of the map. Consequently, nitrogen oxide emissions can be significantly reduced by a reduced pre-chamber enrichment, but also by setting a higher global air excess. In the maps shown in Fig. 3 and 4, this influence is primarily represented by the selection of operating points which are as close as possible to the lean operating limit without violating the stability criterion $COV < 3\%$. This, however, leads to a significant increase in HC emissions and the indicated efficiency decreases by an average of about 0.45 % points across all operating points.

Operation points with highest efficiency with $COV_{p_{mi}} < 3\%$

pre-chamber fuel: CNG, pre-chamber: 4-hole pre-chamber, CR = 13, camshafts: Standard, Tumble-flap position: closed

• measured operation points

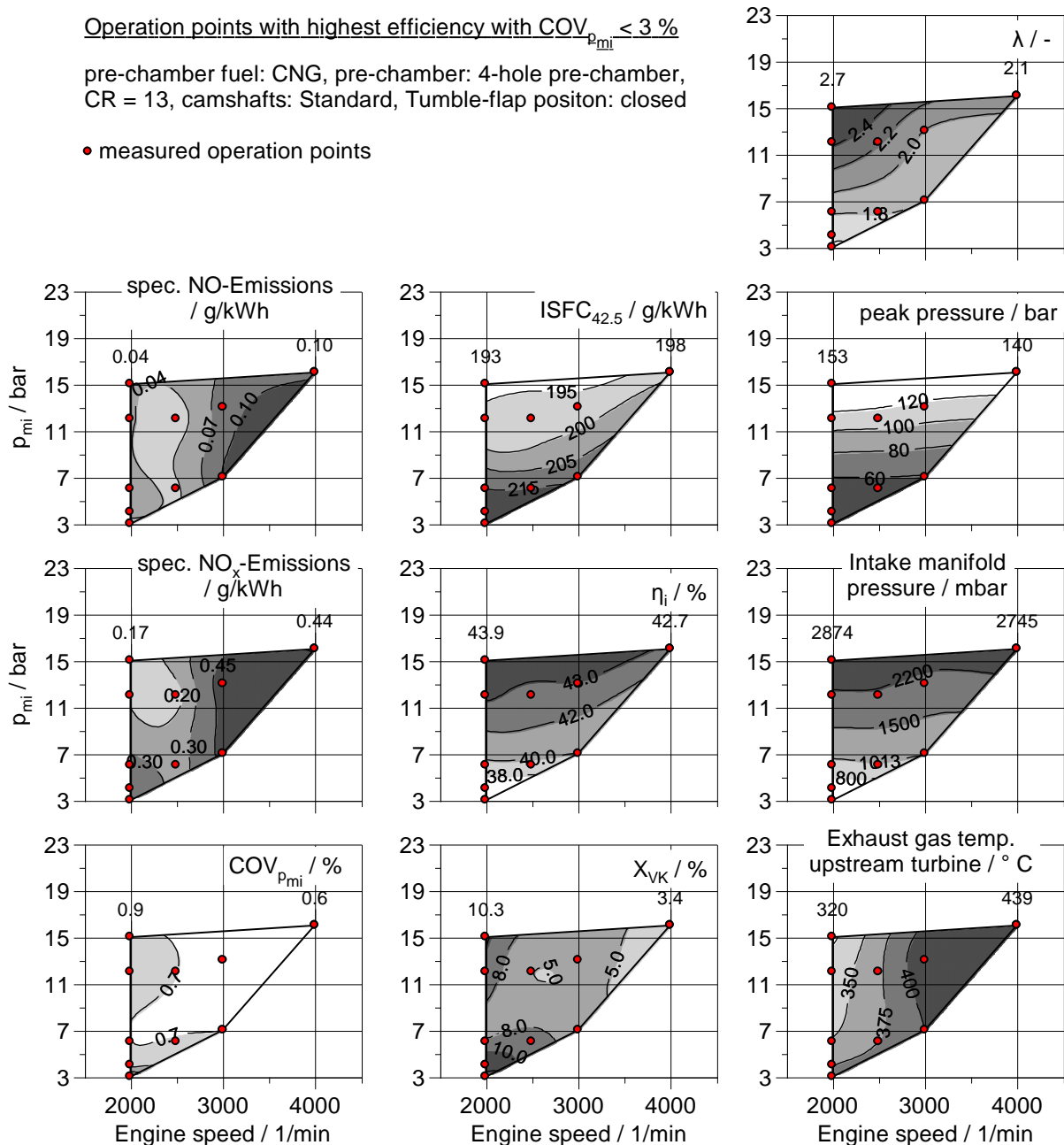


Figure 3 Engine mapping with operation points of highest indicated efficiency in case of natural gas enrichment of a 4-hole pre-chamber

Operation points with lowest NO_x Emissions with COV_{p_{mi}} < 3 %

pre-chamber fuel: CNG, pre-chamber: 4-hole pre-chamber,
CR = 13, camshafts: Standard, Tumble-flap position: closed

• measured operation points

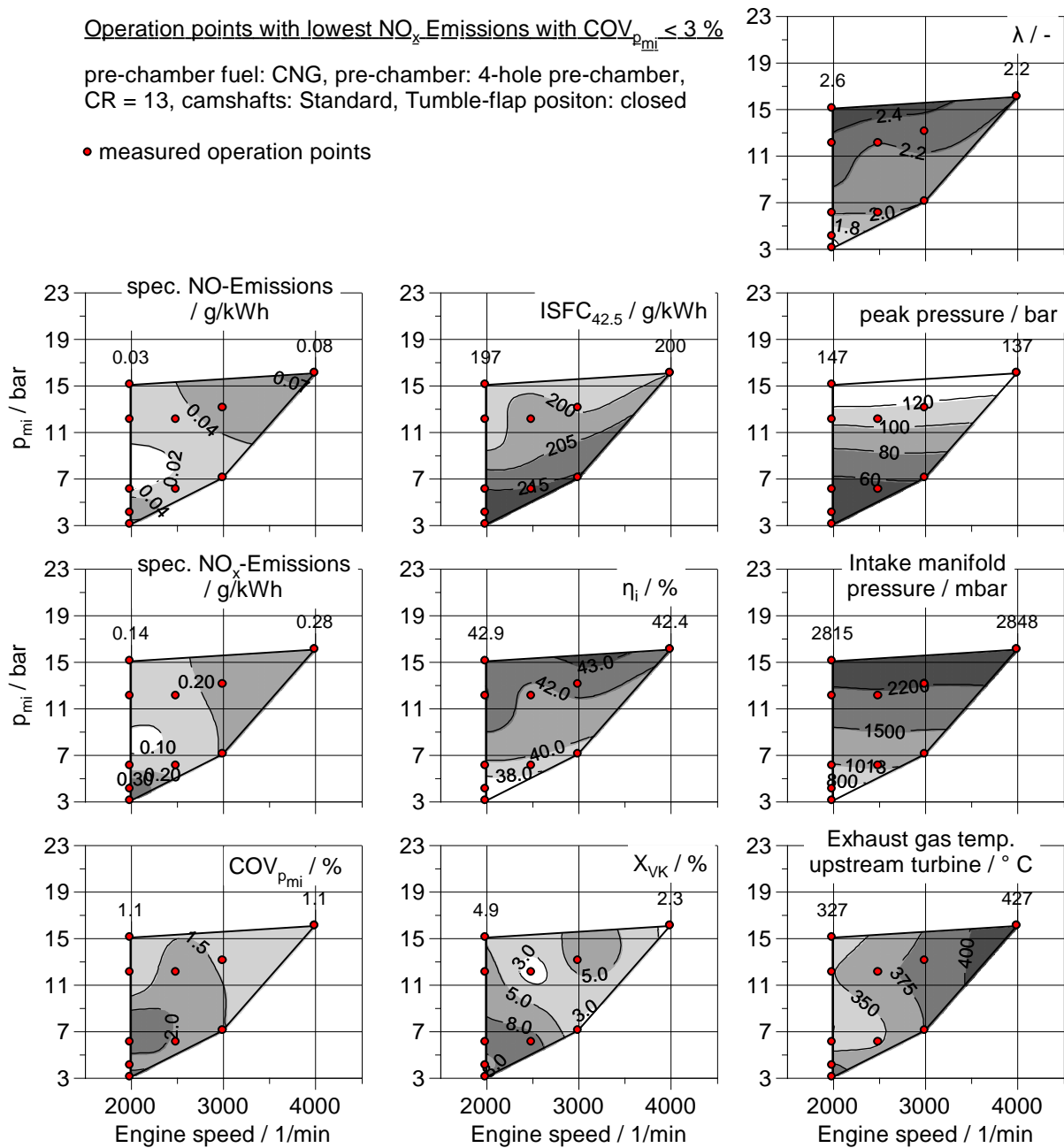


Figure 4: Engine mapping with operation points of lowest nitrogen oxide emissions in case of natural gas enrichment of a 4-hole pre-chamber

Following the discussed lean running limits, the air-fuel ratio for both selection criteria (minimum fuel consumption or minimum nitrogen oxide emissions) shows a very similar, falling curve towards low loads and high speeds. This results in an almost linear increase in boost pressure demand and peak pressure with the load. In order to realize the high loads with a lean combustion relative air-fuel ratio of up to $\lambda = 2.7$, an intake manifold pressure of almost 2900 mbar (absolute) is required. The maximum peak pressure from the two maps averages 500 cycles to 153 bar at $n = 2000$ rpm and $imep = 15$ bar. With values ranging between 320 °C and 439 °C or else between 326 °C and 426 °C, the exhaust gas temperatures before turbine are in a similar range. They increase with engine speed which on the one hand results from a higher power output, and on the other hand also from a lower air excess in the selected operating points. From the analogous correlation follows an exhaust gas temperature that decreases at 2000 rpm with increasing load.

3.3. Optical Investigations

Figure 5 shows images of the combustion chamber for a further operating point created using an 8 mm endoscope to visualize the processes in the combustion chamber in addition to the pressure curves and the characteristic values of the pressure indication. A frame rate of 12 kHz is selected for this observation, whereby a resolution of one image per degree crank angle is achieved at a speed of 2000 rpm.

$n_{Mot} = 2000$ 1/min, IMEP = 15 bar, CR = 13, $SOI_{CC} = 295^\circ$ CA btdc, $SOI_{PC} = 80^\circ$ CA btdc
 $m_{K_VK_Z} = 2.0$ mg/Cycle, $\lambda = 2.4$, Pre-chamber fuel: Gasoline ROZ98, 4-hole pre-chamber
 camshafts: Standard, Tumble-flap position: closed

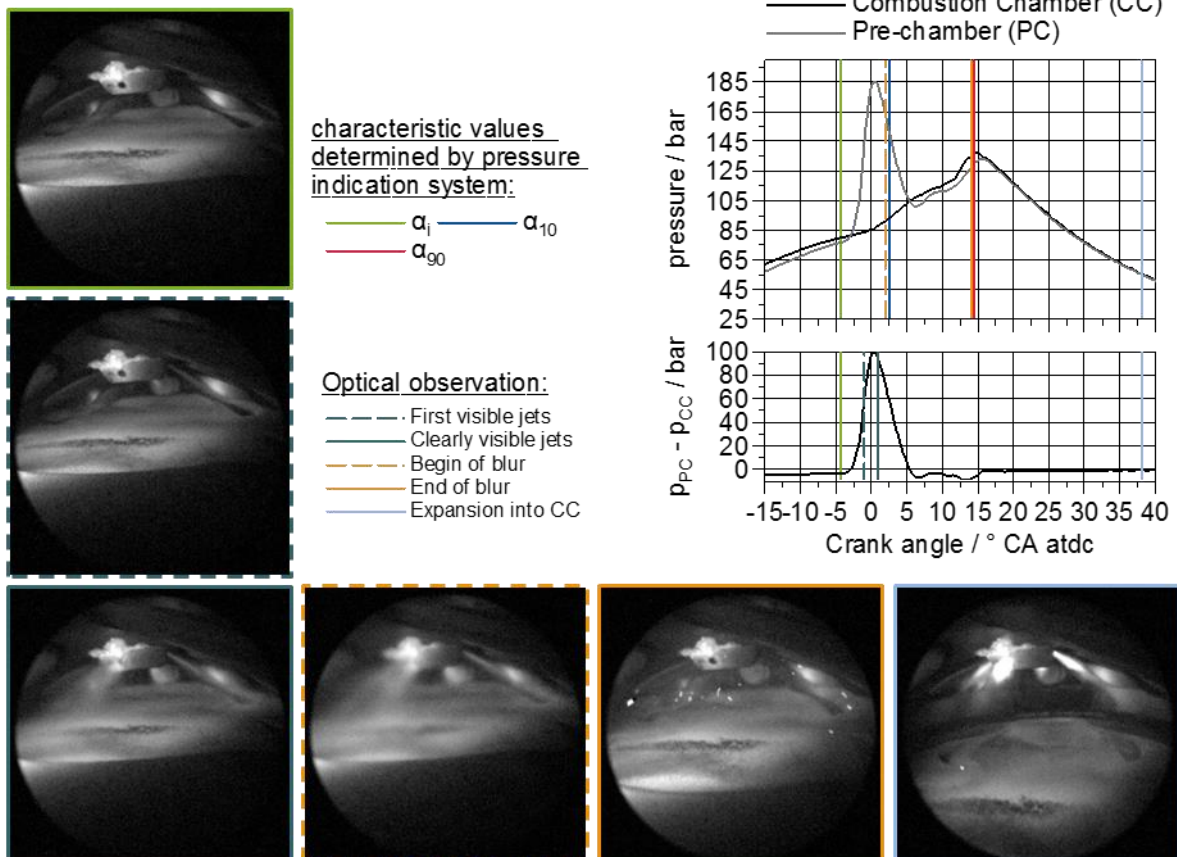


Figure 5: Pressures and optical sequences of the pre-chamber ignition system at $\lambda = 2,4$, $n = 2000$ rpm, imep = 15 bar

While at the point of ignition the pressure in the pre-chamber is lower than the pressure in the combustion chamber due to the throttled inflow into the pre-chamber in the compression phase, the pressure increase in the pre-chamber generates a positive pressure difference to the combustion chamber due to the fuel conversion from approx. 2.5 deg bTDC. At this point, there are no effects visible in the combustion chamber. In the phase of the maximum pressure increase at approximately 1 deg CA bTDC, the first formation of turbulent jets into the combustion chamber can be seen on the images.

In the vicinity of the pressure maximum of the pre-chamber, jets emerging from the jet holes can be very clearly seen. At this point, the main fuel conversion phase in the pre-chamber is completed. Due to the high pressure difference, the pre-chamber mass is blown out into the combustion chamber. During this expansion phase of the pre-chamber, combustion begins in the main combustion chamber. This is shown on the one hand by the combustion chamber indication which yields 10 % of mass fraction burned according to the heat law. On the other hand, the differences in density in the combustion chamber become visible on the combustion chamber image at this point in time.

The resulting fuzziness persists during the combustion and decays at 14 deg CA aTDC. At almost the same time, the heat law of the combustion chamber indication yields 90% burn rate. In the following burned mixture expands from the pre-chamber into the main combustion chamber. In this particular operation point, the overflow of burned mass at 36 deg CA aTDC is clearly visible due to the emitted, luminous particles.

For further investigations of the combustion behavior measurements with an UV endoscope were carried out. Using hydrogen enrichment for the pre-chamber ensures that not soot is formed during combustion in the pre-chamber and thus the turbulent jets exiting the pre-chamber are not containing glowing soot particles. Due to its different orientation of this endoscope a 6-hole pre-chamber has been used, as the jets are not targeting directly to optical access of the cylinder head. The images shown in Figure 6 indicate a similarly good agreement between the indication indices and optical observations. For example, a transition between the penetration of the turbulent jets into the combustion chamber and the start of combustion therein with a small inaccuracy is to be associated with the start of combustion α_{10} . Also, the combustion center correlates quite well with the highest intensity on the images. At the burning end, identified by the indication as α_{90} , also the intensity of the exposure of the combustion chamber pictures decreases significantly.

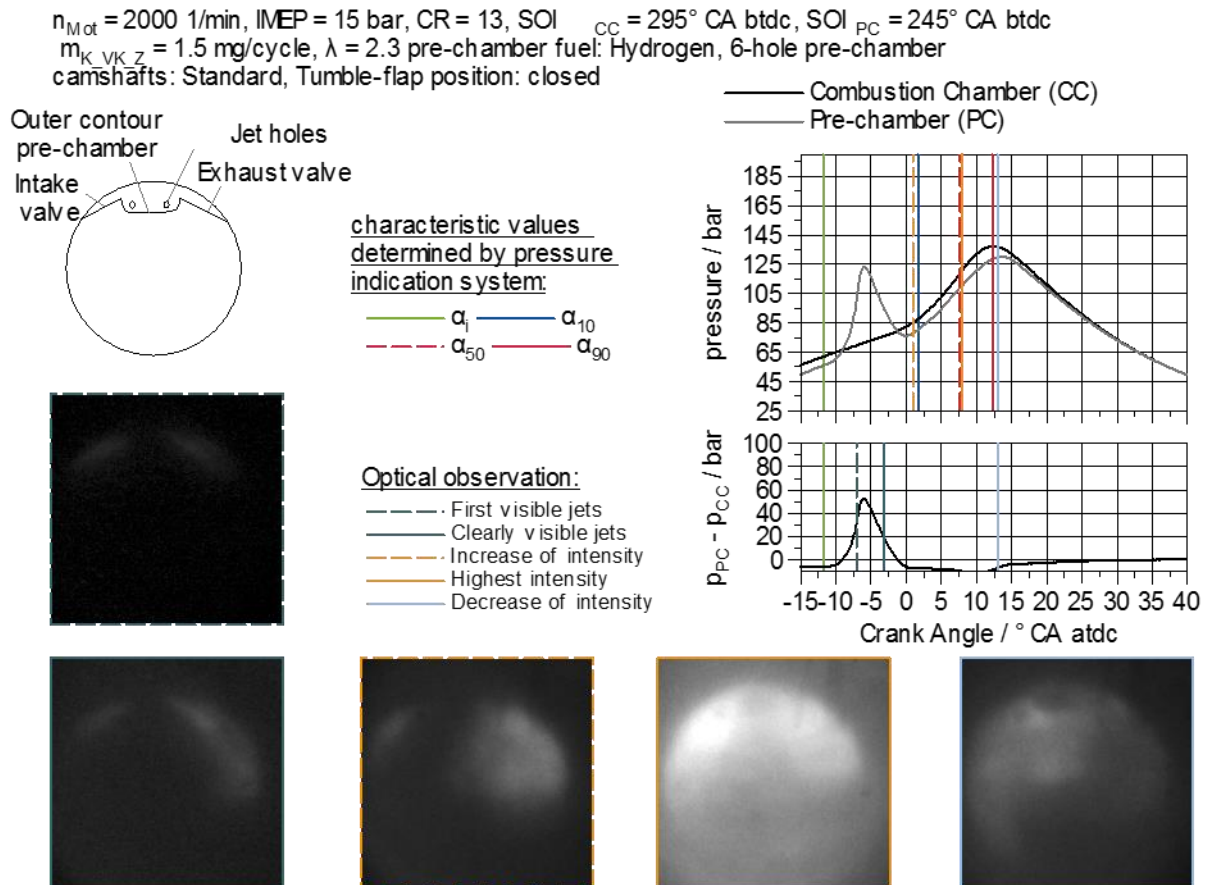


Figure 6: Combustion visualization with UV-transmitting optics

The images also show that the combustion in the main chamber starts along the turbulent jets. However, flame propagation mainly takes place outside at the cylinder walls. Hence, in contrast to conventional spark plug operation, the mixture burns from the outside to the center instead of from the center (spark plug) to the outside. For richer operating points, the combustion process propagating from the outside to the center is more distinct. The results of Kawabata et al. provide an explanation for this behavior. The mixture dilution in the pre-chamber is lower due to the influx of mixture from the combustion chamber during compression, and hence, the spray jets are more intense. They unfold when hitting the combustion chamber walls. This surface enlargement ensures that the combustion takes-off primarily at the outside and only secondarily along the beams. Firstly, an outer ring of the combustion is formed. If the spray jets are less intense such as in leaner operation, they do not penetrate so far into the combustion chamber. Unfolding at the outer cylinder wall is less distinct. The ignition of the mixture along the spray jets becomes the primary ignition mechanism.

4. Summary / Conclusion

Pre-chamber jet ignition represents an attractive approach for a lean burn engine concept in hybridized powertrains. The development of such systems seeks intense frontloading by means of simulation and supportive optical investigations during thermodynamic experimental phase on a single cylinder engine.

The numerical approaches used for the layout, allow for an efficient development process of the pre-chamber by combining approaches with various levels of detail. 0D models based on multi-zone combustion are used to evaluate a broad variety of pre-chamber geometries with respect to the operating conditions, their volumes and hole configuration. The multi-zone combustion model is based on detailed caloric sub-models taking into account the mixture state, thermodynamic boundaries and the transition from laminar to turbulent combustion. This approach is supplemented by the use of reactive 3D computational fluid dynamics, which considers the spatially resolved mixture and turbulence distribution in the pre- and main combustion chamber. Thus, a detailed optimization of the pre-chamber geometry with respect to the combustion quality is realized. Based on this optimization, pre-chambers with different hole number and pattern were realized, tested and evaluated with regard to lean burn capability, efficiency and emissions. Optical investigations serve to conclude on the burn rate and on particulate emission. Furthermore, the effects of liquid vs. gaseous pre-chamber fuels as well as of injection parameters such as e.g. the fuelling ratio of pre-chamber vs. main chamber have been investigated. Having found specific layouts to achieve stable combustion ($COV < 1.5\%$) for homogeneous $\lambda > 3$ operation and specific NO_x emissions below 0.1 g/kWh a synthesis of all findings was made to define the final concept as the best compromise for the required specification. Furthermore, the findings allow to interpret the combustion stability mechanisms at the lean burn limit and to show options for controlling them. The resulting combustion system with its good lean burn capability offers a high efficiency in the entire engine map and thus excellent conditions for further improving the efficiency of electrified powertrains.

Acknowledgements

Project 'EAGLE' has received funding from the European Union's Horizon 2020 research and innovation program under grant agreement No 724084 (<https://h2020-eagle.eu>).

The authors express their thanks to T. Ottenwälder, C. Kupiek and A. Jeckel

Nomenclature

CC	combustion chamber
CA	crank angle
COV	coefficient of variation (here: of IMEP)
CFD	Computational Fluid Dynamics
CR	compression ratio
CRFD	Computational Reactive Fluid Dynamics
IMEP	indicated mean effective pressure
n_{mot}	engine speed
NO	nitrogen oxide
PC	pre-chamber
SOI _{CC}	start of injection combustion chamber
SOI _{PC}	start of injection pre-chamber
$m_{K_VK_Z}$	injected fuel mass into pre-chamber each combustion cycle
α_i	spark timing
α_{10}	10 % mass fraction burnt
α_{50}	50 % mass fraction burnt
α_{90}	90 % mass fraction burnt
λ	relative air-fuel-ratio
k	Turbulent kinetic energy
k_x	Turbulent kinetic energy in geometrical range x
m	mass
m_x	mass in geometrical range x
v_{hole}	velocity in pre-chamber hole

C_{hole}	discharge coefficient of pre-chamber hole
t	Time
s_T	Turbulent combustion velocity
s_L	Laminar Combustion Velocity
Da	Damköhler Number
v'	Turbulent fluctuation velocity
$b1$	Model constant for turbulent combustion approximation
$b3$	Model constant for turbulent combustion approximation
$a4$	Model constant for turbulent combustion approximation

References

- R. Böwing: "Der Einfluß von Zündung und Zylinderinnenströmung auf die Verbrennung in Ottomotoren mit hoher Ladungsverdünnung, Dissertation RWTH Aachen 2000
- M. Bunce, H. Blaxill: "Sub-200 g/kWh BSFC on a Light Duty Gasoline Engine", SAE Technical Paper 2016-01-0709, 2016, doi:10.4271/2016-01-0709
- M. Sens, E. Binder, P.-B. Reinicke, M. Rieß, T. Stappenbeck, M. Wobke: „Die Vorkammerzündung und vielversprechende Komplementär-Technologien“ – 27. Aachener Kolloquium 2018
- M. Schumacher, M. Wensing: "A Gasoline Fuelled Pre-Chamber Ignition System for homogenous Lean Combustion Processes", SAE Technical Paper 2016-01-2176, 2016, doi:10.4271/2016-01-2176
- G. Lumsden, H.C. Watson : "Optimum Control of an S.I. Engine with a $\lambda=5$ Capability", SAE Technical Paper 950689, 1995, doi:10.4271/950689
- Y. Kawabata und D. Mori, „Combustion Diagnostics & Improvement of a Pre-chamber Lean-Burn Natural Gas Engine“ in SAE Technical Paper Series, 2004-01-0979
- M. Auer, S. Blodig and G. Wachtmeister, "Combustion Modelling of Open Chamber and Pre-Chamber Gas Engines". 9th Stuttgarter International Symposium, 2009
- N. Peters, "Turbulent Combustion (Cambridge Monographs on Mechanics)". Cambridge University Press, 2000
- M. Grill, M. Bargende, "Cylinder Module: Development of a highly-modular zero-dimensional engine process calculation code". FVV project no. 869, 2013
- A. Babajimopoulos et al., „A fully coupled computational fluid dynamics and multi-zone model with detailed chemical kinetics for the simulation of premixed charge compression ignition engines“ in International Journal of Engine Research 6, 2005
- D. Serrano, J.-M. Zaccardi, C. Müller, C. Libert and K. Habermann, "Ultra-Lean Pre-Chamber Gasoline Engine for Future Hybrid Powertrains" in SAE ICE 2019 (planned)
- W. Wiese, S. Pischinger, P. Adomeit and J. Ewald, "Prediction of Combustion Delay and -Duration of Homogeneous Charge Gasoline Engines based on In-Cylinder Flow Simulation" in SAE Technical Paper 2009-01-1796, 2009